Published in final edited form as:
J Cell Physiol. 2008 July ; 216(1): 29–37. doi:10.1002/jcp.21426.

Topical Administration of a Multi-Targeted Kinase Inhibitor Suppresses Choroidal Neovascularization and Retinal Edema

John Doukas[1], **Sankaranarayana Mahesh**[1], **Naoyasu Umeda**[2], **Shu Kachi**[2], **Hideo Akiyama**[2], **Katsutoshi Yokoi**[2], **Jon Cao**[1], **Zoe Chen**[1], **Luis Dellamary**[1], **Betty Tam**[1], **Adrienne Racanelli-Layton**[1], **John Hood**[1], **Michael Martin**[1], **Glenn Noronha**[1], **Richard Soll**[1], and **Peter A. Campochiaro**[2,*]

[1]TargeGen, Inc., 9380 Judicial Drive, San Diego, CA, 92121

[2]The Departments of Ophthalmology and Neuroscience, The Johns Hopkins University School of Medicine, Baltimore, Maryland 21287-9277

Abstract

Age-related macular degeneration, diabetic retinopathy, and retinal vein occlusions are complicated by neovascularization and macular edema. Multi-targeted kinase inhibitors that inhibit select growth factor receptor tyrosine kinases and/or components of their down-stream signaling cascades (such as Src kinases) are rationale treatment strategies for these disease processes. We describe the discovery and characterization of two such agents. TG100572, which inhibits Src kinases and selected receptor tyrosine kinases, induced apoptosis of proliferating endothelial cells *in vitro*. Systemic delivery of TG100572 in a murine model of laser-induced choroidal neovascularization (CNV) caused significant suppression of CNV, but with an associated weight loss suggestive of systemic toxicity. To minimize systemic exposure, topical delivery of TG100572 to the cornea was explored, and while substantial levels of TG100572 were achieved in the retina and choroid, superior exposure levels were achieved using TG100801, an inactive prodrug that generates TG100572 by de-esterification. Neither TG100801 nor TG100572 were detectable in plasma following topical delivery of TG100801, and adverse safety signals (such as weight loss) were not observed even with prolonged dosing schedules. Topical TG100801 significantly suppressed laser-induced CNV in mice, and reduced fluorescein leakage from the vasculature and retinal thickening measured by optical coherence tomography in a rat model or retinal vein occlusion. These data suggest that TG100801 may provide a new topically applied treatment approach for ocular neovascularization and retinal edema.

Keywords

age-related macular degeneration; angiogenesis; diabetes; macular edema; Src kinase; vascular endothelial growth factor

INTRODUCTION

Neovascularization and edema are major issues in several ocular diseases, including age-related macular degeneration (AMD), retinal vein occlusions (RVO), and diabetic retinopathy (Campochiaro, 2000; Campochiaro, 2004). Vascular endothelial growth factor (VEGF), a critical stimulus for neovascularization and edema, plays a central role in these

*Corresponding author: Peter A. Campochiaro, M.D., Maumenee 719, The Johns Hopkins University School of Medicine, 600 N. Wolfe Street, Baltimore, MD 21287-9277, Telephone #: (410) 955-5106, Fax #: (410) 614-9315, pcampo@jhmi.edu.

diseases (Campochiaro, 2006). Intraocular injections every 6 weeks of pegaptanib, a pegylated oligonucleotide that selectively binds $VEGF_{165}$, caused a reduction in severe vision loss over 1 year in patients with subfoveal choroidal neovascularization (CNV) due to AMD (Gragoudas et al., 2004). Intraocular injections every month for a year of ranibizumab, an antibody fragment that binds all isoforms of VEGF-A, eliminated severe vision loss in 95% of patients and significantly improved vision in 33–44% of patients (Brown et al., 2006; Rosenfeld et al., 2006) The results with ranibizumab are impressive, because it is the first treatment to cause visual improvement in patients with subfoveal CNV and it is now the standard of care. There is also mounting evidence that VEGF antagonists provide benefit in diabetic macular edema and macular edema due to retinal vein occlusions (Campochiaro et al., 2008; Nguyen et al., 2006)

While the role of VEGF in these disease processes is clear, it is likely that other proteins also contribute. Platelet-derived growth factor-B (PDGF-B) promotes proliferation of vascular endothelial cells and induces the recruitment and survival of pericytes (Hirschi et al., 1999; Lindahl et al., 1997) stabilizing newly developed vessels and rendering them less susceptible to VEGF blockade (Armulik et al., 2005). In both tumor and ocular models of neovascularization, combined blockade of VEGF and PDGF-B is superior to blockade of VEGF alone (Bergers et al., 2003; Jo et al., 2006). Transgenic mice that express high levels of PDGF-B in the retina develop excessive migration and proliferation of pericytes, endothelial cells, and glial cells resulting in severe proliferative retinopathy and retinal detachment (Mori et al., 2002; Seo et al., 2000). The fibroblast growth factor (FGF) family is another group of potent angiogenic factors. Overexpression of FGF2 in the eye does not stimulate neovascularization because it is sequestered (Ozaki et al., 1998; Tobe et al., 1998) but FGF2 does contribute to CNV when there is tissue disruption from the disease process itself or attempts at treatment (Yamada et al., 2000). Therefore, combined blockade of VEGF, PDGF, and FGF receptors may provide greater efficacy for the treatment of ocular neovascularization than targeting VEGF alone.

Similar logic would also support a multi-targeted approach to blocking macular edema. The best choice here may be inhibition at several levels within a single signaling cascade. For example, the Src family kinases c-Src and Yes mediate the vascular permeability-inducing actions of VEGF (Eliceiri et al., 1999), and therefore dual VEGF receptor/Src kinase inhibition would provide a double hit against VEGF-induced edema. Such multiple hits within one signaling cascade are believed to synergize in terms of overall efficacy (de Jonge and Verweij, 2006).

Current protein-based therapies inhibit only VEGF and because of their large size are administered by repeated intraocular injections. Agents that can be delivered by topical administration to the cornea could offer substantial advantages beyond a less invasive delivery mode, for example the potential for a superior safety profile if systemic exposure were meaningfully reduced. The ability of patients to self-medicate would be another advantage. To address these issues of target selection and deliverability, we characterized the preclinical performance of two newly developed small molecule kinase inhibitors, modeling pharmacokinetics in rodents and rabbits as well as efficacy in rodent models of CNV and retinal vein occlusion. The first of these compounds, TG100572, inhibits several growth factor receptors in addition to Src family kinases, and the second, TG100801, is a prodrug version of TG100572 designed for superior pharmaceutical properties.

MATERIALS AND METHODS

Kinase inhibitors

TG100572 (4-chloro-3-(5-methyl-3-{[4-(2-pyrrolidin-1-ylethoxy)phenyl]amino}-1,2,4-benzotriazin-7-yl)phenol) and TG100801 (4-chloro-3-(5-methyl-3-{[4-(2-pyrrolidin-1-ylethoxy)phenyl]amino}-1,2,4-benzotriazin-7-yl)phenyl benzoate) were designed and synthesized at TargeGen. Compounds were prepared for *in vitro* assays as DMSO stocks, for i.p. delivery as Solutol:polyethylene glycol 400:ethanol:water solutions (10:10:10:70, pH 5), and for topical delivery as sterile-filtered aqueous-based solutions containing 1% hydroxypropyl methyl cellulose, 0.2% tyloxapol, 3.4% dextrose, 0.006% benzalkonium chloride, and 0.025% ethylenediaminetetraacetic acid (280 mOsm, pH 5.4). Inhibition of kinase activities were determined using commercial services (Upstate, Charlottesville, VA and InVitrogen, Carlsbad, CA).

Cell-based assays

For proliferation assays, human retinal microvascular EC (Cell Systems, Kirkland, WA) plated in 96-well cluster plates were cultured for 48 hr in the presence of either TG100572 (2 nM-5 μM) or DMSO (vehicle control); medium contained 10% FBS, 50 μg/mL heparin, and 50 ng/mL rhVEGF (Peprotech, Rocky Hill, NJ). Cell numbers were then assessed using an XTT-based assay (Roche, Alameda, CA). For apoptosis assays, human umbilical vein EC maintained in either a proliferating state (medium supplemented with 10% FBS) or a quiescent state (medium with 0.5% FBS) were incubated for 24 hr in the presence of TG100572 (0.4 or 4 μM) or DMSO. Genomic DNA was then isolation using a commercial kit (Gentra Systems, Minneapolis, MN), 5 μg samples electrophoresed on 1.2% agarose gels, and UV-illuminated images acquired using an Alpha Imager system (Alpha Innotech Corp., San Leandro, CA). For Western blot assays, microvascular EC were first incubated overnight in serum and growth factor-free medium, then exposed for 1 hr to 1 μM TG100572. Following a 10 min incubation in medium containing rhVEGF (50 ng/ml), cells were lysed and processed as Western blots to detect phosphorylated Akt kinase or total STAT3 (as a loading control); antibodies were obtained from Cell Signaling Technologies (Danvers, MA).

Pharmacokinetic studies

All animal studies followed current “NIH Guidelines for the Use of Laboratory Animals”, as well as guidelines established by the Association for Research in Vision and Ophthalmology. C57BL/6 mice (15–20 g) were dosed i.p. twice daily for 4 days with 5 mg/kg TG100572, followed by a single dose on Day 5, 5 hr after which plasma samples were taken, animals euthanized, and eyes explanted. Alternatively, mice were dosed topically with either TG100572 or related prodrugs (e.g., TG100801) by delivering a single 10 μL drop to both eyes for a total of two days, and both plasma and eyes harvested prior to or 0.5, 1, 3, 5, or 7 hr after the Day 2 dosing. Dutch-Belted rabbits (1.5–2.5 kg) were dosed topically with 0.6% TG100801 as a single drop in each eye (40 μL drop volume), and 2 hr later plasma and tissues harvested.

Mouse eyes were dissected to yield retinas and eye cups (consisting of sclera with attached choroid), then pooled (N= 2–4) according to tissue type so as to maximize detection sensitivity. For rabbits, eyes were more extensively dissected to yield multiple tissues (cornea, aqueous humor, iris, ciliary body, lens, sclera, choroid, retina, and vitreous humor); in addition, the palpebral conjunctiva was also harvested. After weighing, ocular tissues were homogenized in RIPA buffer using a FastPrep homogenizer (Thermo Scientific, Milford, MA) followed by extraction in acetonitrile (containing internal standards), and then supernatants were dried and reconstituted into DMSO:water (8:2). Plasma samples were

extracted in a 2-fold excess of acetonitrile (containing internal standards) followed by centrifugation to obtain supernatants. Processed plasma and ocular tissue samples were then quantitated by LC/MS/MS against external calibration standards prepared in naïve mouse tissues. The LC/MS/MS system consisted of a Sciex API3000 triple quadrupolar mass spectrometer (MDS Sciex, South San Francisco, CA), an Agilent 1100 HPLC system (Agilent Technologies, Santa Clara, CA), and a CTC autosampler (Leap Technologies, Carrboro, NC). LC separations were performed on a Zorbax SB reverse phase HPLC column (Agilent Technologies); mass spectrometric detection was achieved using electrospray ionization operating in positive ionization mode. Pharmacokinetic parameters were estimated using WinNonlin software (Pharsight, Mountain View, CA) based on mean concentrations for each time point and individual tissue. Maximum concentration (C_{max}) and time to C_{max} (T_{max}) were determined based on measured concentrations; area under the curve (AUC) measurements were calculated from mean concentration data using the linear trapezoidal rule.

Ocular safety assessments

Both gross and slit lamp exams were performed on Dutch Belted rabbits (1.7–2.2 kg) pre-study to establish baselines. Variables assessed included: ocular discharge and discomfort, conjunctival hyperemia and chemosis, corneal transparency and vascularization, lens opacity, iris hyperemia, aqueous and cellular flare, and pupillary response (Hackett and McDonald, 1996). In addition, ERGs (both photopic and scotopic) were performed followed by flicker fusion assessments. Rabbits were then dosed topically four times per day for 28 days with either 1% TG100801 or vehicle, delivered as 40 μL to each eye; this relatively high dosing frequency was selected to produce a high challenge for ocular tolerability. Gross exams were repeated daily and slit lam exams weekly. After a final set of exams on Day 29, ERGs were repeated, animals euthanized, and eyes processed for histopathology.

Ocular distribution of ^{14}C-TG100801

A male Dutch-Belted rabbit (2.1 kg, Myrtle's Rabbitry, Thompson Station, TN) received a single 40 μL topical ocular dose, in the left eye only, of 1% TG100801 containing 25 μCi of ^{14}C-TG100801 (with the ^{14}C label placed on a position retained in TG100572, so that radioactivity would indicate either parent compound TG100801 or TG100572). At 30 minutes post-instillation, approximately 30 mL of blood was collected and the animal was euthanized. The head of the rabbit was immediately frozen in a hexane/dry ice bath and stored at −70°C for 2 hours, after which it was embedded in chilled carboxymethylcellulose and frozen into a block, and then tangentially sectioned onto adhesive tape at 40 μm thickness. Selected sections were dried at −20°C and mounted, and tightly wrapped with Mylar film and exposed on phosphorimaging screens for 4 days. Exposed screens were scanned using an Amersham Biosciences Storm. Blood and plasma were analyzed directly using a Model 2900TR liquid scintillation counter (Packard Instrument Company) with Ultima Gold XR scintillation cocktail.

Mouse model of CNV

CNV was induced by laser photocoagulation-induced rupture of Bruch's membrane as previously described (Tobe et al., 1998). In brief, 5 to 6 week old female C57BL/6 mice were anesthetized with ketamine/xylazine and pupils were dilated with 1% tropicamide. Three burns of 532 nm diode laser photocoagulation (75 μm spot size, 120 mW, 0.1 seconds duration) were delivered to retinas (9, 12, and 3 o'clock positions of the posterior pole) using a slit lamp-mounted OcuLight GL diode laser (Iridex, Mountain View, CA), with a handheld cover slip as a contact lens to view the retina. Only burns in which a bubble was produced (indicating Bruch's membrane rupture) were included on-study. For 14 days following laser treatment, mice were treated systemically with TG100572 (5 mg/mg) or

vehicle via daily i.p. injections. Alternatively, for topical dosing, TG100801 (as a 1 or 0.6% solution) or vehicle was applied twice daily to the eye as 10 μL volumes; slit lamp examinations were used to follow ocular tolerability throughout the study. After 14 days, mice were perfused with 1 mL of PBS containing 50 mg/mL of fluorescein-labeled dextran (2×10^6 average molecular weight, Sigma-Aldrich, St. Louis, MO), eyes were removed and fixed for 1 hour in 10% phosphate-buffered formalin. After dissecting free the cornea, lens, and retina, four radial cuts were made in the eyecup allowing it to be flat mounted in aqueous mounting medium. Flat mounts were then examined by fluorescence microscopy and images were digitized using a three-color CCD video camera and a frame grabber. Image analysis software (Image-Pro Plus, Media Cybernetics, Silver Spring, MD) were then used to measure the total area of choroidal neovascularization at each rupture site by personnel blinded as to study treatments and groups. Additionally, some mice were used for pharmacokinetic analyses as described above rather than for measurement of CNV.

Rat model of retinal vein occlusion

Long Evans rats (250–275 gm) were anesthetized with ketamine/xylazine, and then injected i.v. with Rose Bengal (as a 5% saline solution) at 20 mg/kg. Four minutes later, using a slit lamp-mounted OcuLight GL/GLx 532nm Green laser, (Iridex Corporation, Mountain View, CA) 4–8 low power laser burns (50 μm spot size, 60 mW power, and 0.1 sec duration with 0.4 sec interval) were delivered to induce a thrombus in the single retinal vein in the superior quadrant (1–2 disc diameters from the optic disc) of the right eye; care was taken not to burn the surrounding retina. Approximately 10 min later, vein thrombosis and retinal edema were confirmed by slit lamp exam (thrombosis persisting for several days and not spontaneously resolving until post-Day 3). Animals were dosed topically in both eyes with 10 μL of TG100801 (as a 0.3, 0.6 or 1% solution) or vehicle. A total of 5 topical applications were delivered per eye over a three day period: dosing was performed one hour prior to and six hours after laser-induced thrombosis on Day 1, twice on Day 2, and once the morning of Day 3. One hour after the final topical application, retinal edema was assessed by one of two means.

Retinal edema was quantified by personnel blinded as to study treatments and groups. Animals were first injected i.p. with sodium fluorescein (200 μL of a 10% saline solution). Forty-five minutes later, rats were anesthetized with ketamine/xylazine and a topical anesthetic applied to each eye. A Fluorotron FM-2 ocular fluorophotometer adapted for small laboratory animal optics (OcuMetrics, Mountain View, CA) was then used to detect fluorescein leakage into the retina and posterior chamber. Scans were taken of both eyes, plots generated representing fluorescence along the vertical axis, and from the peak signal in the retina and posterior chamber an Edema Index (EI) was calculated according to the following formula: $EI = (F_{od} - F_{os})/F_{os}$, where F_{od} = AUC value for fluorescence in the right eye, and F_{os} = AUC value for fluorescence in the left (treated but not thrombosed) eye. In this way, thrombosis-induced leakage in the right eye was corrected for background permeability in the same animal's non-thrombosed eye.

Retinal thickness was also used as a measure of retinal edema (as previously by personnel blinded as to study treatments and groups). Rats were anesthetized with ketamine/xylazine and a topical lubricant applied to each eye, after which retinal scans were taken using a Stratus OCT Model 3000 instrument (Zeiss Meditec, Dublin, CA); the Stratus had been adapted for small animal use by adjusting the Z offset (axial position). Scans were taken in the vertical plane so as to cover a 5 mm area extending from the edge of the optic disc (superiorly in the vertical meridian). Scan thickness was then calculated (using the Stratus' internal software) at 6 evenly spaced points along the 5 mm scan.

Statistics

Two group comparisons were made using unpaired Student's t-tests, and multiple group analyses using one-way analyses of variance (ANOVA) with post-hoc Dunnett's tests (SigmaStat software; SPSS, Chicago, IL). If Dunnett's tests showed statistical differences for more than one group as compared to controls, a second ANOVA for inter-group differences was performed using the Student-Newman-Keuls Method as the post-hoc test. Statistical significance was defined as $P < 0.05$.

RESULTS

Biochemical and cellular characterization of a dual receptor tyrosine kinase/Src kinase inhibitor

Exploring a novel series of benzotriazines (Noronha et al., 2006) for activity against both receptor tyrosine kinases (RTK) and Src kinases identified TG100572 as a potential therapeutic candidate, based on its low to sub-nanomolar activity against the Src family as well as RTK such as VEGFR1 and R2, FGFR1 and R2, and PDGFRβ (Table 1). As would be predicted given this profile, TG100572 inhibited vascular endothelial cell proliferation *in vitro* (ED_{50}= 610 ± 71 nM, mean ± SEM, N= 3) and blocked VEGF-induced phosphorylation of extracellular signal-regulated kinase (ERK), a signaling event in VEGF-induced mitogenesis (Meadows et al., 2001) (Fig. 1A). Additionally, TG100572 induced apoptosis in rapidly proliferating, but not quiescent, endothelial cell cultures (Fig. 1B). These data suggest the potential that this kinase inhibitor would target angiogenic but not established blood vessels for growth arrest.

Inhibition of CNV following systemic kinase inhibitor delivery

In order to directly assess the influence of our multi-targeted kinase inhibition approach on ocular neovascularization, we employed a well-established murine model in which laser-induced rupture of Bruch's membrane leads to CNV (Tobe et al., 1998). In this model, edema and neovascularization occur at laser sites within one week. Mice that received daily intraperitoneal injections of TG100572 (5 mg/kg) developed smaller CNV lesions than those seen in vehicle-injected mice; measuring CNV area using image analysis techniques demonstrated a 40% reduction compared to the vehicle control group (Fig. 2A; $P < 0.001$). However, the TG100572-treated group also lost an average 11% of their body weight over the 14 day course of this study compared to the vehicle-treated group which gained an average 1% (Fig. 2B; $P = 0.006$). This weight loss suggests at least some degree of systemic toxicity, in agreement with our starting hypothesis that achieving acceptable therapeutic indices will be challenging with systemic delivery of multi-targeted kinase inhibitors.

To correlate TG100572 concentrations in ocular tissues with the observed CNV reduction effect, eyes from mice dosed by intraperitoneal injection with 5 mg/kg of TG100572 were dissected to yield retina as well as combined sclera/choroid samples, and these samples processed for mass spectroscopy. TG100572 levels were 818 nM in the retina and 9 μM in the choroid/sclera.

Pharmocokinetics and ocular tolerability of TG100572 and the prodrug TG00801

As a means of overcoming toxicity issues associated with systemic delivery of multi-targeted kinase inhibitors, ocular exposure following topical delivery was explored in mice. Delivering TG100572 daily as a single 10 μL drop of a 1% formulation achieved a 24 hr exposure ($AUC_{0–24hr}$) of 6,800 h·nM in the posterior eyecup (combined sclera/choroid/retina). Interestingly, in comparative studies, superior exposure was achieved by topical delivery of prodrug versions of TG100572. The most promising of these, TG100801, achieved approximately 1.7-fold higher TG100572 exposure (11,357 h·nM) than the parent

compound when delivered topically at an equivalent 1% formulation strength (Table 2). Additionally, nearly equivalent TG100801 exposure (9,200 h·nM) was also observed in the posterior eyecup, representing a pool of prodrug for potential conversion to TG100572. Based on these favorable results, TG100801 was selected for further exploration of topical dosing regimes.

TG100801 was formed by derivitization of a phenolic moiety in TG100572 to yield an ester, and of the prodrugs examined, displayed the best balance of stability (physical and chemical) with hydrolysis rate. On its own, TG100801 does not display meaningful anti-kinase activity, as the ester group blocks key interactions with kinase active sites (data not shown), however exposure to esterases (abundant in mammalian tissues) rapidly liberates active TG100572. As shown in Table 2, topically delivery of a 1% formulation achieved maximal TG100572 concentrations (C_{max}) in both the sclera/choroid and retina that were less than those achieved by i.p. administration of 5 mg/kg TG100572, but still well in excess of its biochemical IC_{50} values against RTK and Src kinases. Time to maximal TG100572 concentrations (T_{max}) was relatively rapid (1 hr), but exposure was also relatively durable, as indicated by the $AUC_{0–24hr}$ measures. By contrast, plasma concentrations of both TG100801 and TG100572 remained below the level of detection (2 nM) at all time points examined; these multi-log differences between ocular and plasma concentrations suggest minimal potential for systemic toxicity.

Similar pharmacokinetic profiles were seen in rats as that observed in mice (Table 2); the clearest differences were higher concentrations of TG100801 vs. TG100572 in the rat, indicating a more gradual conversion of prodrug to active form in this species. To follow in more detail the route by which topically applied TG100801 reaches the posterior segment, in this case using a 0.6% formulation, rabbits were used to enable a finer dissection of ocular tissues (Table 3). As would be expected, given the topical route of administration, the highest concentration of TG100801 was found at the front of the eye (conjunctiva and cornea); TG100572 concentrations were even higher, indicating a rapid de-esterification of the prodrug in these tissues. TG100572 also predominated in the posterior segment (relative to TG100801), where both compounds established a gradient from the exterior to interior compartment: sclera > choroid > retina > vitreous humor. This gradient, coupled with the near absence of TG100801 and TG100572 in the aqueous humor and lens, suggests a trans-scleral (as opposed to trans-corneal) route of delivery to the posterior segment (Hughes et al., 2005). This is supported by the observation that, although both molecular species were detected in the iris and ciliary body, concentrations were lower than those seen in the sclera and choroid; trans-corneal diffusion should have resulted in higher levels. The absence of detectable TG100801 or TG100572 plasma concentrations also argues against a systemic delivery route (where topically applied compound accesses the systemic circulation and thereafter accumulates in the posterior segment). Finally, the predominance of TG100572 over TG100801 in most compartments, the reverse of the general trend seen in the rodent studies presented in Table 2, may have resulted from a longer contact time of the prodrug with a larger eye, or simply reflect that a lower concentration of TG100801 (0.6%) was used in the rabbit studies (the larger tissue volumes reducing the need for a loading dose), allowing for more efficient conversion of prodrug.

Rabbits were also used to more closely assess tolerability and safety following TG100801 topical application. Despite pushing exposure via an aggressive dosing schedule (1% TG100801 delivered four times per day for 28 days), TG100801 was judged well-tolerated. Daily gross exams and weekly slit lamp exams did not detect ocular changes beyond baseline responses (Hackett and McDonald, 1996) and histopathology revealed normal ocular histology at study end. Additionally, electroretinograms (ERG) taken pre- and post-study revealed no meaningful changes, confirming normal retinal health and function at

study end. As for systemic effects, animals did not lose weight during the study course and showed no gross signs of systemic toxicity (data not shown).

Topical administration of ^{14}C-TG100801 in the rabbit

In order to further explore the route by which TG100801 and TG100572 achieve posterior ocular tissue exposure following topical administration, a radiotracer study was conducted in a Dutch-Belted rabbit. Compound was delivered as a single unilateral (left eye) topical instillation of 1% TG100801 containing ^{14}C-TG100801. At 30 minutes post-instillation, there was considerable local absorption of radioactivity into ocular tissues of the dosed eye with no observed contralateral exposure (Figure 3). Radioactivity outlined the globe anteriorly and posteriorly as a relatively thick band suggesting penetration into the sclera. No radioactivity was detected within the lens, vitreous, iris, ciliary body, or optic nerve head. The majority of tissues within the head were also negative for radiotracer signal, most notably the vascular system, which coupled with an absence of detectable radioactivity in plasma samples (as determined using a liquid scintillation counter) indicate minimal systemic exposure. Radioactivity was noted in the nasolacrimal duct, the nasal turbinates, the eyelids, and the exterior fur of the nose outlining the drainage, through the nasolacrymal duct. These radioactive tracer data agree with the pharmacokinetic data presented in Tables 2 and 3.

Topical administration of a TG100801 suppresses CNV

Our pharmacokinetic and radiotracer data suggest that topical delivery of TG100801 represents a viable means of delivering active compound to the posterior segment. The effect of this delivery on a pathologic process was tested using the murine model of laser-induced CNV described above. Mice received twice a day topical administration of vehicle alone or containing 0.6% or 1% TG100801.. Fluorescent photomicrographs of FITC-perfused choroidal flat mounts suggested reduced CNV at sites of Bruch's membrane rupture in both TG100801-treated groups (Fig. 4A). Quantification of CNV area confirmed that the 1% TG100801 group showed a 58% reduction relative to the vehicle group (Fig. 4B, P= 0.036). The lower strength TG100801 formulation showed a trend that was not statistically significant (43% reduction, P= 0.057). Slit lamp examinations showed that both formulation strengths were well tolerated with no signs of irritation, inflammation, or other ocular toxicity, and no signs of systemic toxicity were seen.

Topical administration of a TG100801 suppresses retinal edema

As the laser-induced CNV model clearly established the ability of a topically applied RTK/Src kinase inhibitor to reduce neovascularization in the subretinal space, we next sought to determine whether retinal pathologies could also be successfully treated. For this goal we utilized a rat model of retinal vein occlusion, in which animals are injected i.v. with a photosensitive dye (Rose Bengal) followed by relatively low-energy laser application so as to induce thrombosis of a single retinal vein. Slit lamp exams as well as fluorescein angiography confirmed a rapid onset of edema in the ischemic territory, beginning within minutes and persisting approximately one week. Pilot studies also confirmed that this edema resulted from retinal ischemia, rather than laser injury, as it only developed in animals pre-injected with Rose Bengal, and could be blocked by anticoagulation so as to prevent thrombus formation (data not shown).

Fluorescein leakage from the retinal vasculature was used as the first measure of edema. Ocular fluorophotometry measures fluorescein in the retina and vitreous as an initial single peak, followed by a later aqueous chamber peak located to the right (Fig. 5). TG100801 markedly reduced the area covered by the retina/vitreous peak. Maximal efficacy was achieved using as low a formulation strength as 0.3%, as application of either 0.3% or 1%

TG100801 formulations produced statistically equivalent reductions in edema vs. vehicle-treated animals (47%, P= 0.002, and 32%, P = 0.039, respectively).

In a separate study, optical coherence tomography (OCT) was used as a second measure of retinal edema; group comparisons were made between naive (non-thrombosed) eyes and thrombosed eyes treated with either vehicle or 1% TG100801. Visually, OCT scans showed considerable retinal thickening and cystic change at Day 3 post-thrombosis in the vehicle-treated group (Fig. 6). In contrast, TG100801-treated eyes showed less prominent thickening and no obvious cysts or subretinal fluid. Figure 6D shows retinal thickness measurements taken at multiple points along 5 mm OCT scans; TG100801 reduced retinal thickness to a statistically significant degree vs. vehicle-dosed animals at 5 out of 6 points (15–26% reduction, P< 0.05). Naive animals showed an average retinal area of 203 ± 2 μm^2 in the region encompassed by the scans compared to 327 ± 23 μm^2 in the thrombosed, vehicle-treated group and 257 ± 13 μm^2 in the thrombosed TG100801-treated group (a 21% reduction vs. the vehicle-treated group, P= 0.013).

DISCUSSION

Neovascular age-related macular degeneration, proliferative diabetic retinopathy and macular edema due to diabetic retinopathy or retinal vein occlusions differ in terms of initiating events and anatomic localization, but each involves visual loss due to leakage from pre-existent or new vessels resulting in collections of fluid within or under the macula. VEGF is a major stimulus in each of these disease processes, but other growth factors are also involved. We hypothesized that a multi-targeted approach to kinase inhibition could provide broadly-based blockade of these pathologies, one potentially more comprehensive than that achievable by targeting a single initiating factor (such as VEGF) or a single event in their signaling cascades (such as ligand-receptor interaction). Additionally, through a medicinal chemistry approach we also aimed for a goal that to date has been a difficult to achieve, obtaining therapeutic levels in the posterior segment after topical (rather than intraocular or systemic) delivery.

Multi-targeted kinase inhibitors have been recognized for their value in oncology, showing an efficacy advantage by blocking multiple effectors or else blocking a single effector along several points in its signaling pathway (de Jonge and Verweij, 2006). We identified one such molecule, TG100572, that potently inhibits VEGF, PDGF, and FGF receptor tyrosine kinases as well as the Src family of kinases that lie downstream of these receptors. TG100572 blocked proliferation and induced apoptosis of cycling vascular endothelial cells *in vitro*, and suppressed CNV. However, while inhibiting multiple molecules involved in vascular proliferation and leakage is appealing from the standpoint of efficacy, it increases the chances of systemic toxicity. In fact, with systemic administration of TG100572, we observed significant body weight loss suggesting toxicity. This caused us to study local delivery, and while TG100572 achieved substantial levels in the choroid and retina after topical administration to the cornea, higher levels of TG100572 were achieved after topical administration of a pro-drug, TG100801, while minimizing systemic exposure. Topical administration of TG100801 suppressed CNV at Bruch's membrane rupture sites in mice and significantly reduced retinal edema in rats with retinal vein occlusions, all without observable safety issues. These data suggest a therapeutic approach of topical application of TG100801 for vascular diseases of the retina or choroid.

Achieving efficacious drug concentrations in posterior segment tissues is generally considered a technical challenge, particularly when using a topical delivery route. This ability of TG100572 and TG100801 reflects their favorable pharmaceutical properties that also contribute to a favorable therapeutic index. TG100801, while lacking anti-kinase

activity of its own, quickly generated active TG100572 within the eye upon topical delivery. However, neither compound was detectable in the plasma, indicating that delivery to the eye occurred by local penetration and not by systemic absorption. This was supported by the results of radioactive tracer studies, which showed radioactivity highlighting and penetrating the wall of the eye anteriorly and posteriorly with no detectable radioactivity in the systemic circulation or contralateral eye. A common route by which drugs delivered to the cornea enter the circulation is by passing through the nasolacrymal ducts to the nasopharynx and then absorption in the digestive tract. After delivery of radiolabeled TG100801 to the cornea, radioactivity was detected in the nasolacrymal ducts and nasopharynx, but this did not lead to systemic exposure. This is consistent with the observations that neither TG100801 nor TG100572 have any oral bioavailability (oral administration does not result in detectable levels in the circulation) and both are rapidly cleared after intravenous administration (data not shown). These characteristics which are often considered disadvantageous are in fact assets for limiting systemic exposure after topical administration to the eye. Taken together, the pharmacokinetic and radiotracer studies suggest that TG100801 and TG100572 enter the posterior segment by a transcleral route, because 30 minutes after administration of radiolabeled TG100801, radioactivity was seen in and around the posterior sclera with no signal in the anterior segment and substantial levels of both compounds were detectable in the choroid and retina. The presence of TG100801 in these target tissues suggests a possible depot effect from ongoing generation of active TG100572 from tissue stores of TG100801.

The transcleral route extends from sclera to choroid to retina, and thus delivery to the retina is the greatest challenge for topically delivered compounds that follow this path. Importantly, topically applied TG100801 was able to significantly inhibit retinal edema in a rat retinal vein occlusion model. Plasma leakage was directly demonstrated by monitoring fluorescein passage out of the retinal circulation using ocular fluorophotometry, a powerful but infrequently used measure in rodent models. A second endpoint, OCT, was also utilized in the vein occlusion model. This technique is infrequently used in rodent studies due to the technical challenges presented by small rodent eyes. However, when successfully applied in animal models, OCT is an extremely valuable tool as it measures retinal thickness (Fukuchi et al., 2001; Horio et al., 2001; Sho et al., 2005), the critical consequence of excessive vascular permeability and a frequently used endpoint in clinical trials.

While topical administration has been extensively used for glaucoma treatments, in which the target is the trabecular meshwork, there is little precedence for its use in the treatment of posterior segment diseases. The only other published example of a compound that inhibits retinal and choroidal neovascularization after topical administration to the eye is the nonsteroidal anti-inflammarory drug nepafenac (Takahashi et al., 2003).. To our knowledge, our data using TG100801 represent the first report of a topically-applied kinase inhibitor that achieves therapeutic efficacy in the choroid and retina. Our data suggest that topical delivery of a multi-targeted kinase inhibitor to the eye is a viable approach for posterior segment diseases.

REFERENCES

Armulik A, Abramsson A, Betsholtz C. Endothelial/pericyte interactions. Circ Res 2005;97:512–523. [PubMed: 16166562]

Bergers G, Song S, Meyer-Morse N, Bersland E, Hanahan D. Benefits of targeting both pericytes and endothelial cells in the tumor vasculature with kinase inhibitors. J Clin Invest 2003;111:1287–1295. [PubMed: 12727920]

Brown DM, Kaiser PK, Michels M, Soubrane G, Heier JS, Kim RY, Sy JP, Schneider S, Group AS. Ranibizumab versus verteporfin for neovascular age-related macular degeneration. N Eng J Med 2006;355:1432–1444.

Campochiaro PA. Retinal and choroidal neovascularization. J Cell Physiol 2000;184:301–310. [PubMed: 10911360]

Campochiaro PA. Ocular neovascularisation and excessive vascular permeability. Expert Opin Biol Ther 2004;4:1395–1402. [PubMed: 15335307]

Campochiaro PA. Molecular targets for retinal vascular diseases. J Cell Physiol 2006;210:575–581. [PubMed: 17133346]

Campochiaro PA, Hafiz G, Shah SM, Nguyen QD, Ying H, Do DV, Quinlan E, Zimmer-Galler I, Haller JA, Solomon S, Sung JU, Hadi Y, Janjua KA, Choy DF, Arron JR. Ranibizumab for macular edema due to retinal vein occlusions; implication of VEGF as a critical stimulator. Molec Ther. 2008 In press.

de Jonge MJ, Verweij J. Multiple targeted tyrosine kinase inhibition in the clinic: all for one or one for all? Eur J Cancer 2006;42:1351–1356. [PubMed: 16740386]

Eliceiri BP, Paul R, Schwartzberg PL, Hood JD, Leng J, Cheresh DA. Selective requirement for Src kinases during VEGF-induced angiogenesis and vascular permeability. Mol Cell 1999;4:915–924. [PubMed: 10635317]

Fukuchi T, Takahashi K, Shou K, Matsumura M. Optical coherence tomography (OCT) findings in normal retina and laser-induced choroidal neovascularization in rats. Graefes Arch Clin Exp Ophthalmol 2001;239:41–46. [PubMed: 11271460]

Gragoudas ES, Adamis AP, Cunningham ET Jr, Feinsod M, Guyer DR. Pegaptanib for neovascular age-related macular degeneration. N Eng J Med 2004;351:2805–2816.

Hackett, RB.; McDonald, TO. Assessing ocular irritation. In Dermatoxicology. Philadelphia: Taylor & Francis; 1996.

Hirschi KK, Rohovsky SA, Beck LH, Smith SR, D'Amore PA. Endothelial cells modulate the proliferation of mural cell precursors via platelet-derived growth factor-BB and heterotypic cell contact. Circ Res 1999;84:298–305. [PubMed: 10024303]

Horio N, Kachi S, Hori K, Okamoto Y, Yamamoto E, Terasaki H, Miyake Y. Progressive change of optical coherence tomography scans in retinal degeneration slow mice. Arch Ophthalmol 2001;119:1329–1332. [PubMed: 11545639]

Hughes PM, Olejnik O, Chang-Lin JE, Wilson CG. Topical and systemic drug delivery to the posterior segments. Adv Drug Deliv Rev 2005;57:2010–2032. [PubMed: 16289435]

Jo N, Mailhos C, Ju M, Cheung E, Bradley J, Nishijima K, Robinson GS, Adamis AP, Shima DT. Inhibition of platelet-derived growth factor B signaling enhances the efficacy of anti-vascular endothelial growth factor therapy in multiple models of ocular neovascularization. Am J Pathol 2006;168:2036–2053. [PubMed: 16723717]

Lindahl P, Johansson BR, Leveen P, Betsholtz C. Pericyte loss and microaneurysm formation in PDGF-B-deficient mice. Science 1997;277:242–245. [PubMed: 9211853]

Meadows KN, Bryant P, Pumiglia K. Vascular endothelial growth factor induction of the angiogenic phenotype requires Ras activation. J Biol Chem 2001;276:49289–49298. [PubMed: 11682481]

Mori K, Gehlbach P, Ando A, Dyer G, Lipinsky E, Chaudhry AG, Hackett SF, Campochiaro PA. Retina-specific expression of PDGF-B versus PDGF-A: vascular versus nonvascular proliferative retinopathy. Invest Ophthalmol Vis Sci 2002;43:2001–2006. [PubMed: 12037011]

Nguyen QD, Tatlipinar S, Shah SM, Haller JA, Quinlan E, Sung J, Zimmer-Galler I, Do DV, Campochiaro PA. Vascular endothelial growth factor is a critical stimulus for diabetic macular edema. Am J Ophthalmol 2006;142:961–969. [PubMed: 17046701]

Noronha G, Barrett K, Cao J, Dneprovskaia E, Fine R, Gong X, Gritzen C, Hood J, Kang X, Klebansky B, et al. Discovery and preliminary structure-activity relationship studies of novel benzotriazine based compounds as Src inhibitors. Bioorg Med Chem Lett 2006;16:5546–5550. [PubMed: 16931012]

Ozaki H, Okamoto N, Ortega S, Chang M, Ozaki K, Sadda S, Vinores MA, Derevjanik N, Zack DJ, Basilico C, Campochiaro PA. Basic fibroblast growth factor is neither necessary nor sufficient for

the development of retinal neovascularization. Am J Pathol 1998;153:757–765. [PubMed: 9736026]

Rosenfeld PJ, Brown DM, Heier JS, Boyer DS, Kaiser PK, Chung CY, Kim RY, Group MS. Ranibizumab for neovascular age-related macular degeneration. N Eng J Med 2006;355:1419–1431.

Seo M-S, Okamoto N, Vinores MA, Vinores SA, Hackett SF, Yamada H, Yamada E, Derevjanik NL, LaRochelle W, Zack DJ, Campochiaro PA. Photoreceptor-specific expression of PDGF-B results in traction retinal detachment. Am J Pathol 2000;157:995–1005. [PubMed: 10980138]

Sho K, Takahashi K, Fukuchi T, Matsumura M. Quantitative evaluation of ischemia-reperfusion injury by optical coherence tomography in the rat retina. Jpn J Ophthalmol 2005;49:109–113. [PubMed: 15838726]

Takahashi K, Saishin Y, Saishin Y, Mori K, Ando A, Yamamoto S, Oshima Y, Nambu H, Melia MB, Bingaman DP, Campochiaro PA. Topical nepafenac inhibits ocular neovascularization. Invest Ophthalmol Vis Sci 2003;44:409–415. [PubMed: 12506103]

Tobe T, Ortega S, Luna JD, Ozaki H, Okamoto N, Derevjanik NL, Vinores SA, Basilico C, Campochiaro PA. Targeted disruption of the *FGF2* gene does not prevent choroidal neovascularization in a murine model. Am J Pathol 1998;153:1641–1646. [PubMed: 9811357]

Yamada H, Yamada E, Kwak N, Ando A, Suzuki A, Esumi N, Zack DJ, Campochiaro PA. Cell injury unmasks a latent proangiogenic phenotype in mice with increased expression of FGF2 in the retina. J Cell Physiol 2000;185:135–142. [PubMed: 10942527]

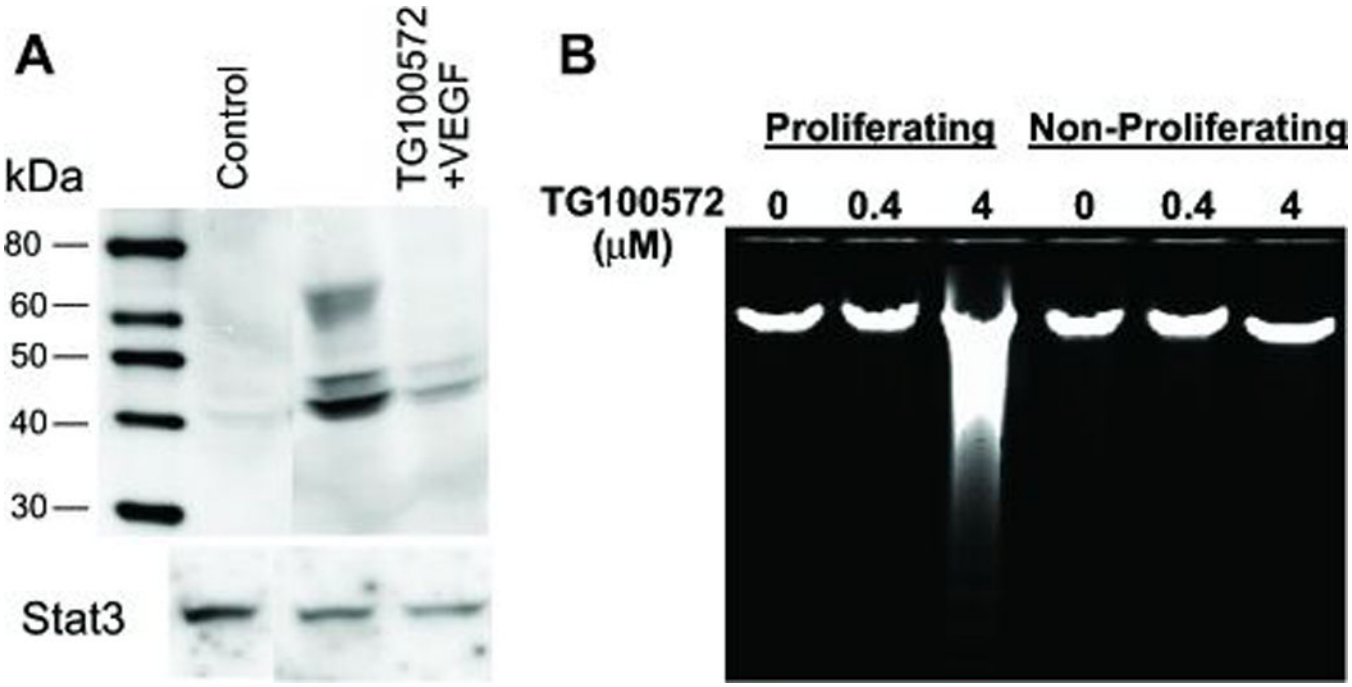

Figure 1. TG100572 inhibits VEGF signaling and induces apoptosis in proliferating vascular endothelial cells

(A) Endothelial cells cultured in the absence of VEGF (Control), in the presence of VEGF, or in the presence of both VEGF and TG100572 were processed for Western blot detection of phosphorylated Erk1/2 (or total STAT3 as a loading control). (B) Endothelial cells cultured under either proliferating (low density/high serum) or non-proliferating (high density/low serum) conditions were exposed to TG100572 at the indicated concentrations for 24 hr, after which genomic DNA was extracted and resolved on agarose gels in order to visualize DNA laddering indicative of apoptosis.

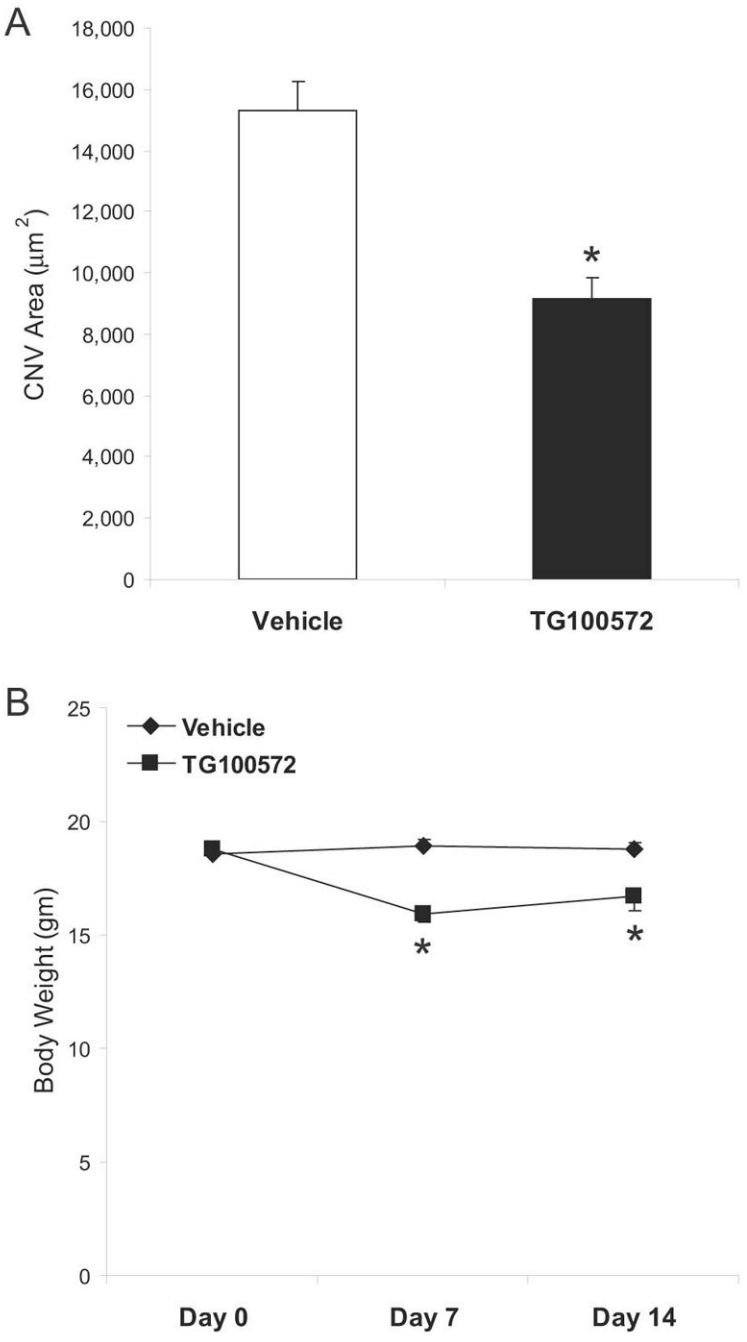

Figure 2. Systemic delivery of TG100572 in a murine model of choroidal neovascularization (CNV)

(A) Laser-induced rupture of Bruch's membrane was performed in C57BL/6 mice, after which animals were dosed i.p daily with either TG100572 (5 mg/kg) or vehicle. After 14 days, animals were perfused with FITC-dextran and choroidal whole mounts were photographed for measurement of CNV area by computerized image analysis (data shown as means ± SEM, n= 55–60 lesion sites; * vehicle and TG100572 groups differ with $P< 0.001$). (B) Body weights taken prior to study initiation, Day 7, and at study end are shown (means ± SEM, n= 11–12 animals; *Vehicle and TG100572 groups differ with $P< 0.005$).

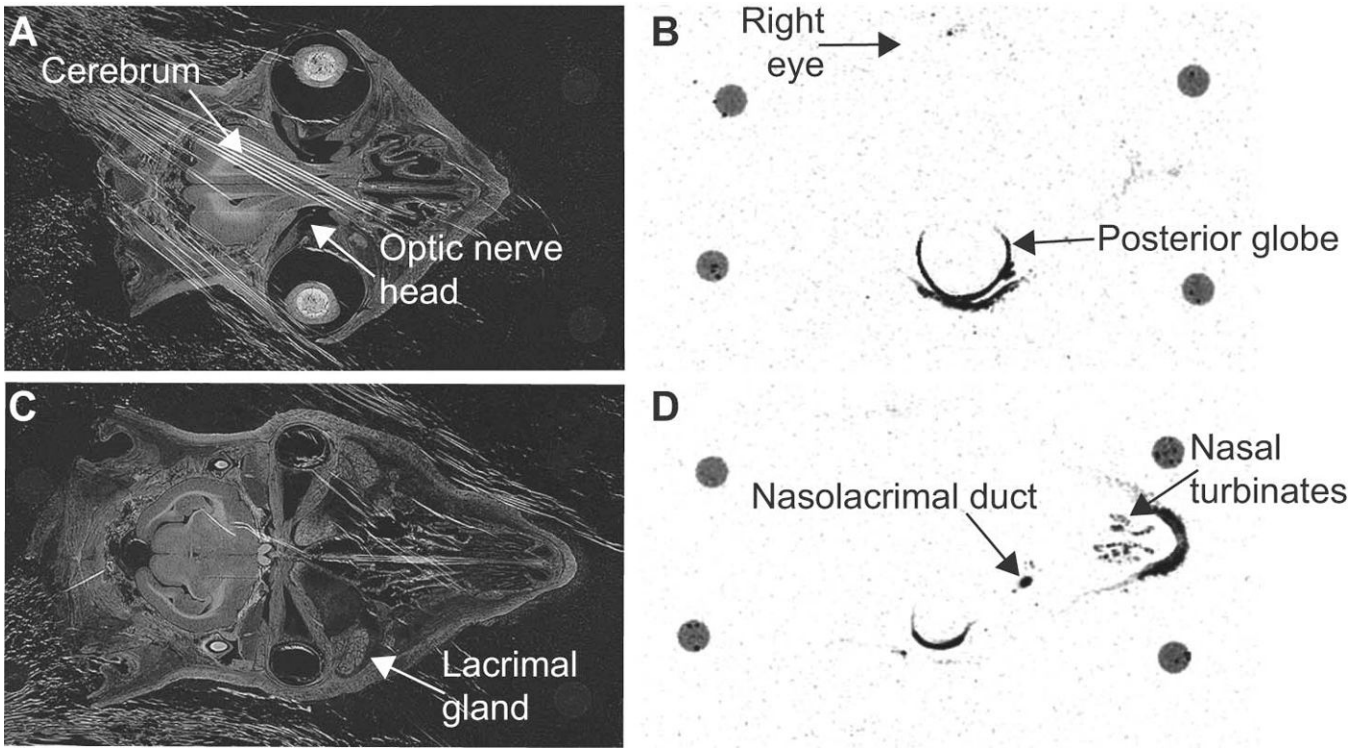

Figure 3. Ocular distribution of ^{14}C-TG100801 following topical instillation in the rabbit

Transillumination (A & C) and corresponding autoradiograph (B & D) images of cross sections through a rabbit's head taken 30 minutes after a single unilateral (left eye) topical instillation of 1% TG100801 containing radiotracer levels of ^{14}C-TG100801. A 40 μm section at the horizontal midline (A & B) or inferior to the midline capturing the nasolacrimal duct (C & D). The four circles visible at the perimeter of each tissue section are remnants of mounting posts.

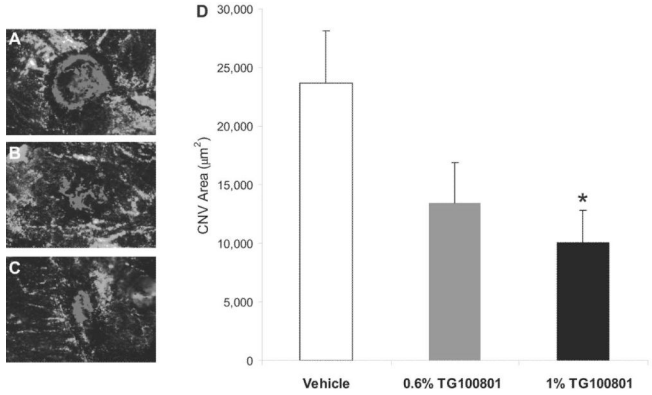

Figure 4. Topical delivery of TG100801 in a murine model of choroidal neovascularlization (CNV)

Laser-induced rupture of Bruch's membrane was performed in C57BL/6 mice, after which animals were dosed topically twice a day with either TG100801 (1% or 0.6% formulations) or vehicle. After 14 days, animals were perfused with FITC-dextran and choroidal whole mounts were photographed for measurement of CNV area by computerized image analysis. (A–C) Representative fluorescent photomicrographs taken from the three treatment groups (A= vehicle, B= 0.6% TG100801, C= 1% TG100801), with fluorescence of the CNV highlighted in red. (D) CNV area graph (data shown as means ± SEM, n= 24 lesion sites; * 1% TG100801 and vehicle groups differ with P= 0.036).

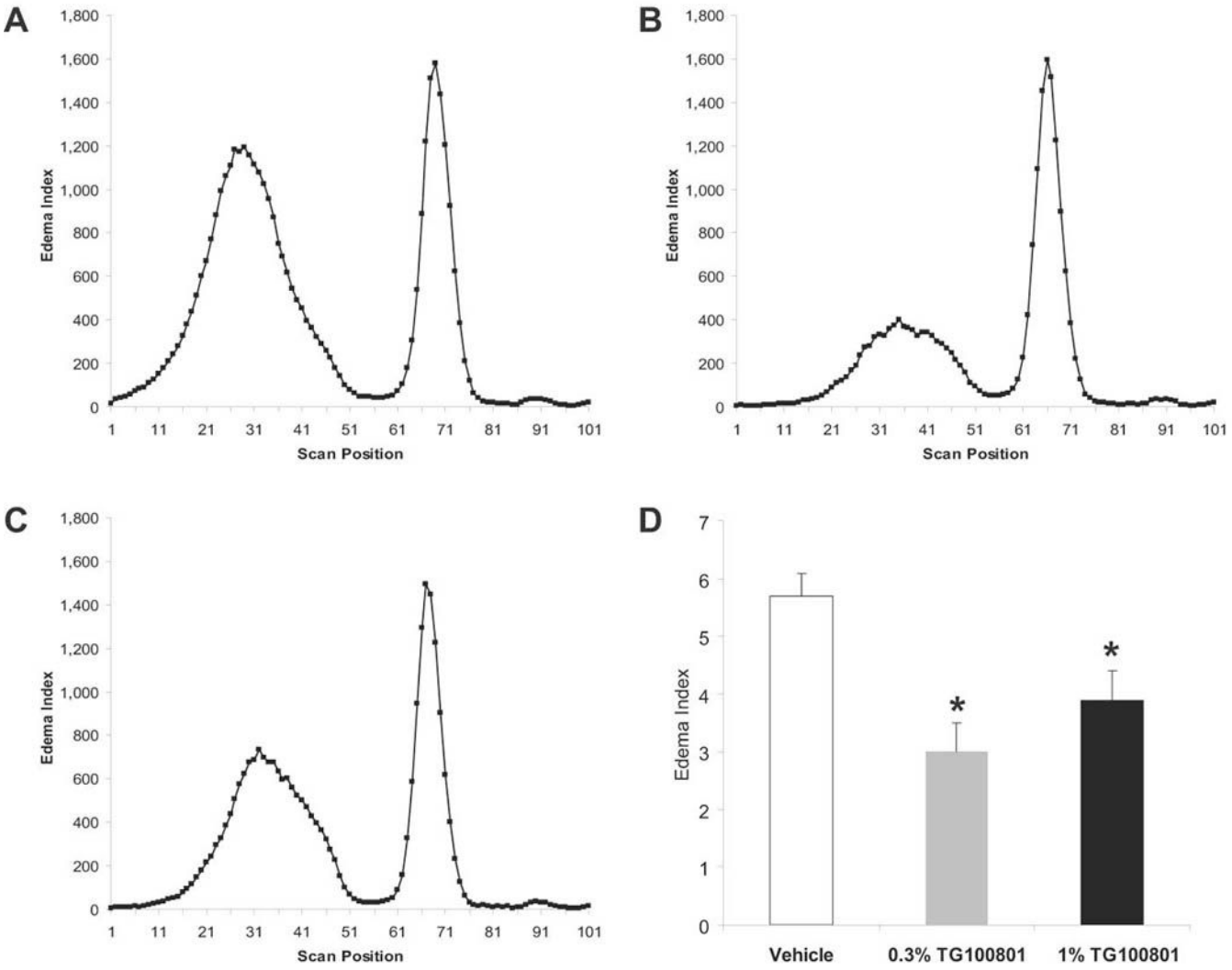

Figure 5. Fluorescein leakage after topical delivery of TG100801 in a rat model of retinal vein occlusion

Retinal vein thrombosis was induced in the right eye of Long Evans rats, and both eyes were dosed topically twice a day with either vehicle or TG100801 (1% or 0.3% formulations). Following 5 doses, animals were injected i.p. with fluorescein and leakage into the retina and vitreous was quantified by ocular fluorophotometry. (A–C) Representative scans taken along the vertical axis from the three treatment groups; the peaks on the left represent fluorescein within the retina and vitreous compartments (A= vehicle, B= 0.3% TG100801, C= 1% TG100801) (D) Retina/vitreous peak area shown as an Edema Index corrected for basal vascular permeability in the non-thrombosed left eye (means ± SEM, n= 9–11; *, both TG100801 groups differ from vehicle group with $P < 0.04$).

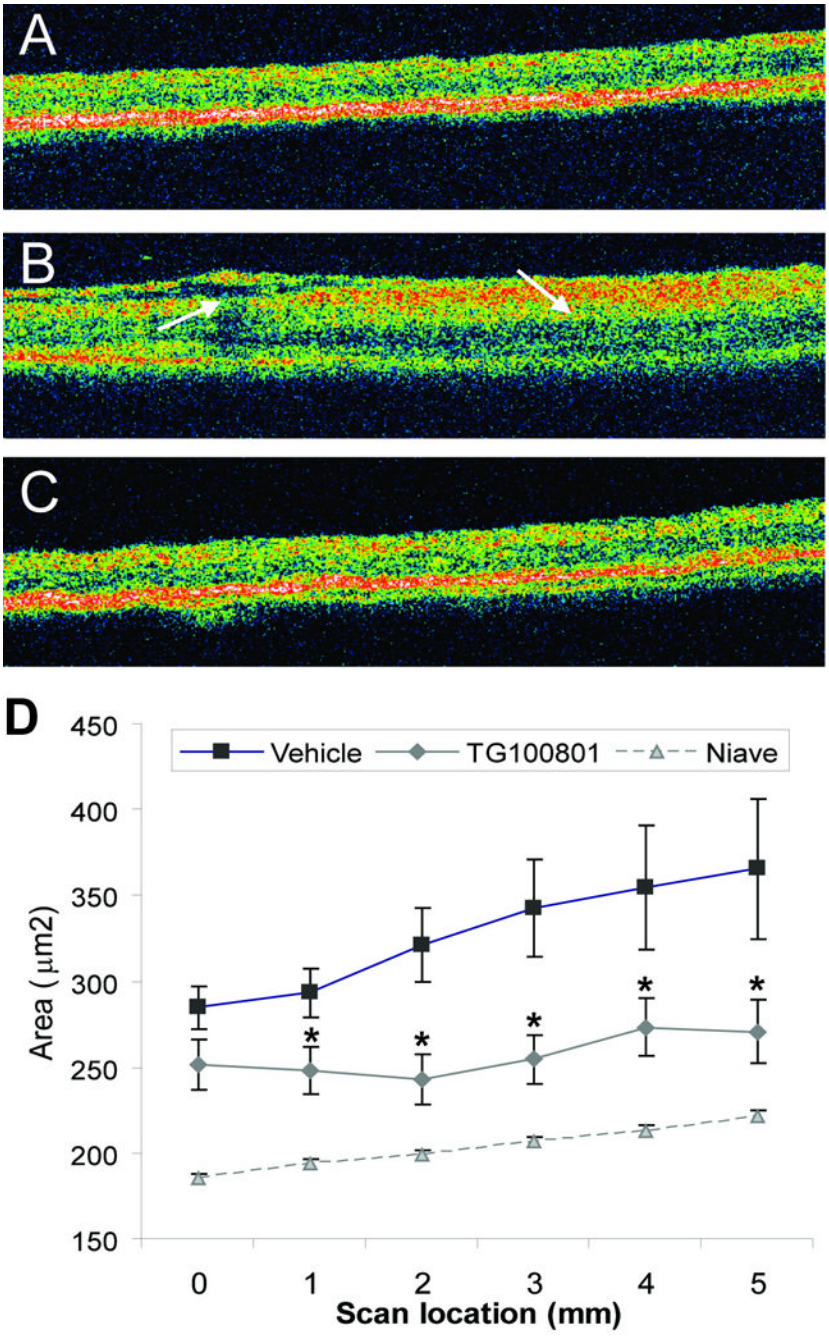

Figure 6. Retinal thickness after topical delivery of TG100801 in a rat model of retinal vein occlusion

A retinal vein occlusion study was performed as described in Fig. 5, except that only one dose of TG100801 (1%) was investigated, and at study end retinal thickness was measured by optical coherence tomography (OCT; A–C). Representative OCT scans taken from naïve (A), thrombosed, vehicle-treated (B), or thrombosed, 1% TG100801-treated (C) animals. (D) Retinal area (μm^2) determined from six 5 mm OCT scans (means ± SEM, n= 17–21; * TG100801 group differs from vehicle group with $P< 0.05$).

Table 1

Kinase inhibitory profile of TG100572

Kinase Family	Kinase	IC_{50} (nM)
Receptor tyrosine kinases	VEGFR1	2
	VEGFR2	7
	FGFR1	2
	FGFR2	16
	PDGFRβ	13
Src family kinases	Fgr	5
	Fyn	0.5
	Hck	6
	Lck	0.1
	Lyn	0.4
	Src	1
	Yes	0.2

The ability of TG100572 to inhibit receptor tyrosine kinases and Src kinase activity was determined in kinase assays as described in Methods. The mean concentrations at which half of maximal inhibition occurred (IC_{50}) were calculated from 3 independent experiments.

Table 2

Pharmacokinetics of topically delivered TG100801 in rodents

Species	PK parameter	TG100801			TG100572		
		Retina	Sclera/ Choroid	Plasma	Retina	Sclera/ Choroid	Plasma
Mouse	C_{max} (nM)	242	1,680	<LOD	97	2,460	<LOD
	T_{max} (h)	1	1	NA	0.5	1	NA
	C_{24hr} (nM)	16	26	<LOD	31	59	<LOD
	$AUC_{(0–24hr)}$ (h·nM)	1,070	8,130	NA	657	10,700	NA
Rat	C_{max} (nM)	607	2,630	<LOD	68	426	<LOD
	T_{max} (h)	1	1	NA	1	1	NA
	C_{24hr} (nM)	7	843	<LOD	5	14	<LOD
	$AUC_{(0–24hr)}$ (h·nM)	2,205	13,090	NA	225	2,840	NA

C57BL/6 mice and Long Evans rats were dosed topically with a single 10 μL drop of 1% TG100801 and at several time points after dosing, tissue and plasma samples were analyzed by mass spectroscopy to determine concentrations of TG100801 and TG100572. The maximal concentration (C_{max}), time to maximal concentration (T_{max}), concentration (C_{24hr}), and 24 hr exposure ($C_{0–24hr}$). Assay level of detection (LOD) was 1 ng/mL (<2 nM). NA: not applicable.

Table 3

Pharmacokinetics of topically delivered TG100801 in rabbits

Tissue	Concentration (nM)			Ratio TG100801: TG100572
	TG100801	TG100572	Sum	
Conjunctiva	609	3,980	4,589	1:6.5
Cornea	38	3,280	3,318	1:86
Aqueous humor	0.5	0	0.5	NA
Iris	9	45	54	1:5
Ciliary Body	65	73	138	1:1.1
Lens	<LOD	<LOD	NA	NA
Sclera	100	249	349	1:2.5
Choroid	34	169	203	1:5
Retina	46	41	87	1:0.9
Vitreous humor	11	11	22	1:1
Plasma	<LOD	<LOD	NA	NA

Dutch Belted rabbits were dosed topically with a single 40 μL drop of 0.6% TG100801 and 2 hours later they were euthanized and ocular tissues were dissected and homogenized. Mass spectroscopy was used to measure the concentrations of TG100801, TG100572, or both (sum) in tissue homogenates. Assay level of detection (LOD) was 1 ng/mL (<2 nM). NA: not applicable.